4D profile of phase objects through the use of a simultaneous phase shifting quasi-common path interferometer

2011 J. Opt. 13 115502

(http://iopscience.iop.org/2040-8986/13/11/115502)

J. Opt. **14** (2012) 019601 (1pp) doi:10.1088/2040-8978/14/1/019601

Erratum

4D profile of phase objects through the use of a simultaneous phase shifting quasi-common path interferometer

Noel-Ivan Toto-Arellano, David Ignacio Serrano-García, Amalia Martínez García, Gustavo Rodríguez Zurita and Areli Montes-Pérez

2011 *J. Opt.* **13** 115502
Received 31 October 2011
Published 23 December 2011

Some equations were incorrect. Corrected equations are presented in this paper.

1. Page 2, section 2, equation (2)

In equation (2), the argument of the Bessel functions was missing. The correct equation is presented below:

$$\tilde{G}(x,y) = \sum_{q=-\infty}^{q=\infty}\sum_{r=-\infty}^{r=\infty} J_q(2\pi A_g)J_r(2\pi A_g) \times \delta(x - qX_0, y - rX_0). \quad (2)$$

2. Page 3, section 2, equation (5)

Equation 5 has errors. The correct equation is presented below:

$$\begin{aligned}\vec{O}'(x,y) &= \vec{O}(x,y) * \tilde{G}(x,y)\\ &= \vec{J}_L \sum_{q,r}^{\infty} J_q J_r \cdot A(x-(q+1/2)x_0, y - rx_0)\\ &+ \vec{J}_R \sum_{q',r'}^{\infty} J_{q'} J_{r'} \cdot B(x-(q'+1/2)x_0, y - r'x_0)\\ &= \sum_{q=-\infty}^{\infty}\sum_{r=-\infty}^{\infty} \{\vec{J}_L J_q J_r + \vec{J}_R J_{q+1} J_r\\ &\times e^{[i\phi(x-(q+1/2)x_0, y-rx_0)]}\}. \quad (5)\end{aligned}$$

3. Page 4, figure 3 caption

Units of the separation x_0 are incorrect. The correct values must be (c) $x_0 = 18$ mm and (d) $x_0 = 26$ mm, or (c) $x_0 = 1.8$ cm and (d) $x_0 = 2.6$ cm.

This correction also applies when figures 3(c) and (d) are referred to in the text. See page 4, left column, lines 4 and 6.

4D profile of phase objects through the use of a simultaneous phase shifting quasi-common path interferometer

2011 J. Opt. 13 115502

(http://iopscience.iop.org/2040-8986/13/11/115502)

IOP Publishing Journal of Optics
J. Opt. **13** (2011) 115502 (8pp) doi:10.1088/2040-8978/13/11/115502

4D profile of phase objects through the use of a simultaneous phase shifting quasi-common path interferometer

Noel-Ivan Toto-Arellano[1], David Ignacio Serrano-García[2], Amalia Martínez García[2], Gustavo Rodríguez Zurita[1] and Areli Montes-Pérez[1]

[1] Laboratorio de Óptica Física, Facultad de Ciencias Físico-Matemáticas de la Benemérita, Universidad Autónoma de Puebla, Pue, Mexico
[2] Centro de Investigaciones en Óptica AC, Loma del Bosque #115, Col. Lomas del Campestre, CP 37150, León, Gto, Mexico

E-mail: ivantotoarellano@cio.mx and david@cio.mx

Received 21 May 2011, accepted for publication 26 September 2011
Published 20 October 2011
Online at stacks.iop.org/JOpt/13/115502

Abstract
Modulation of polarization is commonly employed in optical interferometry through the use of polarizers and quarter-wave retarders. Phase shifts between interfering beams can be easily controlled with such techniques. This communication describes some details of modulation of polarization which are useful in phase shifting interferometry applied to the study of phase objects. As an application, the case of a two-beam phase grating interferometer is discussed on the grounds of polarization analysis as an example. The configuration presented does not require micro-polarizer arrays or additional software to eliminate noise caused by vibration. This system does not use a double window, and generates two beams, the separation of which can be varied according to the characteristics of the grid used. Experimental results are also given.

Keywords: image processing, dynamic interferometry, gratings, phase-shifting, instrumentation, measurement and metrology, polarization, fringe analysis

S Online supplementary data available from stacks.iop.org/JOpt/13/115502/mmedia

(Some figures in this article are in colour only in the electronic version)

1. Introduction

Phase shifting techniques are often used in optical interferometry [1, 2], digital holography [2–4], electronic speckle pattern interferometry and shearography [5–8] because they allow one to analyze samples using non-contact techniques with high accuracy. The use of phase shifting modulated by polarization has the advantage of not requiring mechanical components, such as PZT, to obtain the phase shifts, since it decreases the sensitivity of the system against external vibrations. A common optical system uses linear polarizing filters and birefringent quarter-wave plates to achieve modulation [9–15].

In this paper we propose a quasi-common-path interferometer based on a Mach–Zehnder (MZ) configuration using simultaneous phase shifting interferometry modulated by polarization that shows insensitivity against external vibration. Due to the fact that a MZ system is capable of obtaining two beams, it can be used to implement a common path interferometer that allows the measurement of dynamic events with high accuracy. The configuration presented does not require items such as micro-polarizers [16] but only conventional polarizers, nor does it need additional software to eliminate noise caused by vibration, as the two-beam interferometer is stable. Unlike previously proposed interferometers [11], this system does not use a double window (which should also have a separation x_0 given by the characteristics of the grid used), but it generates two beams whose separation can be varied according to the characteristics of the grid used to obtain the interference patterns. The system implemented is a two-beam phase grating interferometer (TBPGI) modulated by polarization, of which

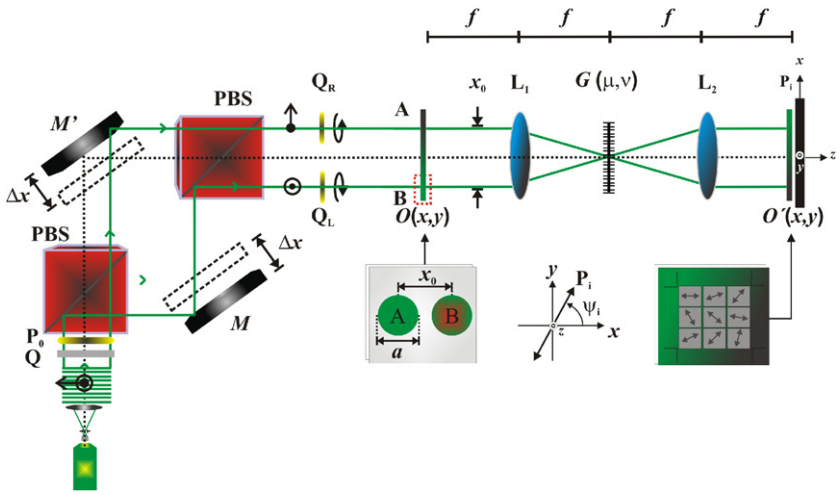

Figure 1. Simultaneous phase shifting quasi-common-path interferometer with modulation of polarization: PBS, polarizing beam splitter; $O(x, y)$, object plane; $O'(x, y)$, image plane; L_i, lens; $G(\mu, \upsilon)$, phase grid; P_i, polarizers; ψ_i, polarizing filter transmission angle; beam transversal section $a = 5$ mm; grating period $d = 110$ lines mm^{-1}; $x_0 = 10$ mm; $f = 150$ mm. Retarding plate operating at $\lambda_0 = 514.5$ nm, retardation $\alpha' = 1.519$ rad.

a detailed description is presented in the following sections. Experimental results for static and dynamic events for phase objects are also presented.

2. Experimental setup

A combination of a quarter-wave plate Q and a linear polarizing filter P_0 generates linearly polarized light oriented at $\pm 45°$ entering the MZ system from a YVO_3 laser operating at 532 nm (see figure 1). This configuration generates two symmetrically displaced beams (beam displacement is larger than beam size $\boldsymbol{a}$) by moving mirrors M and M', enabling one to change the spacing x_0 between the beam centers. Retardation plates with mutually orthogonal fast axes (Q_L and Q_R) are placed in front of beams A and B to generate left and right nearly circular polarized light, respectively [15–18]. The transparent sample is collocated on B, and A is used as a reference beam.

A phase grid carefully constructed by superposing two commercially available phase gratings with their respective grating vectors at $\pm 90°$ is placed at the system's Fourier planes as the pupil. Diffraction orders appear on the image plane, forming a rectangular array. Around each order, an interference pattern appears due to the optical fields associated with each beam when proper matching conditions are met. The interference patterns arise due to the superposition of the diffraction patterns generated by each beam. Taking the rulings of one grating along the μ direction, and the rulings of the second grating along the ν direction, the resulting centered phase grid can be written as

$$G(\mu, \upsilon) = \mathrm{e}^{\mathrm{i}2\pi A_g \sin[2\pi \cdot X_0 \mu]}\, \mathrm{e}^{\mathrm{i}2\pi A_g \sin[2\pi \cdot X_0 \upsilon]} = \sum_{q=-\infty}^{\infty} J_q(2\pi A_g)\, \mathrm{e}^{\mathrm{i}2\pi \cdot qX_0\mu} \sum_{r=-\infty}^{\infty} J_r(2\pi A_g)\, \mathrm{e}^{\mathrm{i}2\pi \cdot rX_0\upsilon}, \quad (1)$$

with $2\pi A_g$ being the grating phase amplitude, and J_q and J_r the Bessel functions of the first kind of integer order q, r, respectively. $\mu = u/\lambda f$ and $\upsilon = v/\lambda f$ are the frequency coordinates scaled to the relevant wavelength and the focal length f. X_0 is the separation of two neighboring diffraction orders in the image plane. The Fourier transform of the phase grid becomes

$$\tilde{G}(x, y) = \sum_{q=-\infty}^{q=\infty} \sum_{r=-\infty}^{r=\infty} J_q(2\pi A_g)\, J_r \times (2\pi A_g)\delta(x - qX_0, y - rX_0), \quad (2)$$

which consists of point-like diffraction orders distributed on the image plane on the nodes of a lattice.

3. Fringe modulation and contrast in phase grating interferometry

Phase grid interferometry is based on a two crossed phase grating placed as the pupil in a 4-f Fourier optical system. A convenient window pair for a grating interferometer implies a vectorial amplitude transmittance given by

$$\vec{O}(x, y) = \vec{J}_L \cdot A\left(x + \frac{x_0}{2}, y\right) + \vec{J}_R B\left(x - \frac{x_0}{2}, y\right), \quad (3)$$

where x_0 is considered as the mutual separation between the centers of each window along the coordinate axis, with an arbitrary retardation α' and the Jones vectors, $\vec{J}_L$ and $\vec{J}_R$, defined as

$$\vec{J}_L = \begin{pmatrix} 1 \\ \mathrm{e}^{\mathrm{i}\alpha'} \end{pmatrix}, \qquad \vec{J}_R = \begin{pmatrix} 1 \\ \mathrm{e}^{-\mathrm{i}\alpha'} \end{pmatrix}. \quad (4)$$

One beam aperture can be described as $A(x, y)$ and the second one as $B(x, y) = \mathrm{e}^{\mathrm{i}\phi(x,y)}$, representing a relative phase between both windows described by $\phi(x, y)$. As shown in figure 1, placing a grating of spatial period $d = \lambda f/x_0$ on the Fourier plane, the corresponding transmittance is given by $G(\mu, \upsilon)$. The image $\vec{O}'(x, y)$ formed by the system consists

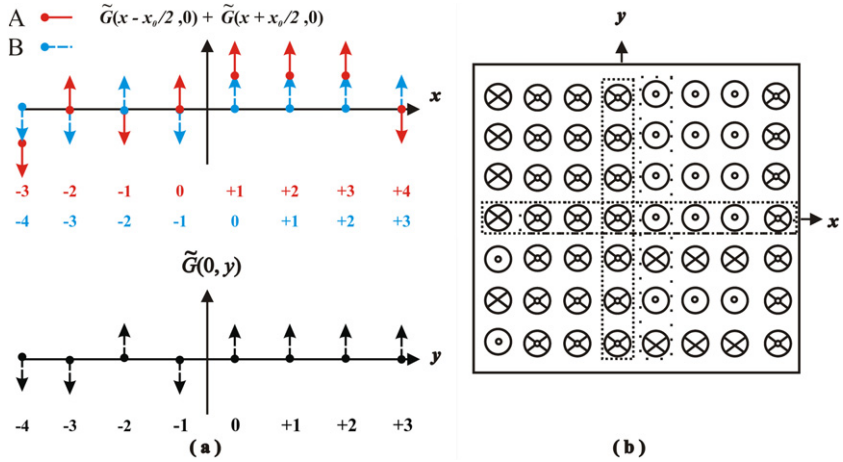

Figure 2. 2D spectra of identical phase gratings to be crossed in order to construct a grid. (a) Theoretical amplitude signs of diffraction orders, resulting from window displacement of $\pm x_0/2$. (b) π-phase distribution of diffraction orders. Dashed lines enclose diffraction orders of indices $(0, n)$ or $(m, 0)$.

basically of replications of each window at distances X_0; that is, the convolution of $\vec{O}(x, y)$ with the Fourier transform of the phase grating. Invoking the condition of matching first-neighboring orders, $X_0 = x_0$, $q' = q + 1$ and $r' = r$, the image is then basically described by

$$\begin{aligned}\vec{O}'(x, y) &= \overleftarrow{O}(x, y)\tilde{G}(x, y)\\ &= \vec{J}_{\mathrm{L}} \sum_{q,r}^{\infty} J_q J_r \cdot A(x - (q + 1/2)x_0, y - rx_0)\\ &\quad + \vec{J}_{\mathrm{R}} \sum_{q',r'}^{\infty} J_{q'} J_{r'} \cdot B(x - (q' + 1/2)x_0, y - r'x_0)\\ &= \sum_{q=-\infty}^{\infty} \sum_{r=-\infty}^{\infty} \{\vec{J}_{\mathrm{L}} J_q J_r + \vec{J}_{\mathrm{R}} J_{q+1}\\ &\quad \times J_r \cdot \mathrm{e}^{[\mathrm{i}\phi(x-(q+1/2)x_0, y-rx_0)]}\}. \end{aligned} \tag{5}$$

By selecting the diffraction term of order qr, after placing a linear polarizing filter with the transmission axis at an angle ψ, $\vec{P}_\psi$, its irradiance results as proportional to

$$\begin{aligned}&\left\| \vec{J}'_{\mathrm{L}} J_q J_r + \vec{J}'_{\mathrm{R}} J_{q+1} J_r \cdot \mathrm{e}^{\mathrm{i}\phi(x', y')} \right\|^2\\ &= A(\psi, \alpha') \cdot [(J_q J_r)^2 + (J_{q+1} J_r)^2\\ &\quad + 2J_q J_r^2 J_{q+1} \cdot \cos[\xi(\psi, \alpha') - \phi(x', y')]] \end{aligned} \tag{6}$$

where x' and y' are the coordinates of the image plane,

$$\begin{gathered}\vec{P}_\psi = \begin{pmatrix} \cos^2\psi & \sin\psi\cos\psi \\ \sin\psi\cos\psi & \sin^2\psi \end{pmatrix},\\ \vec{J}_{\mathrm{L}'} = \vec{P}_\psi \vec{J}_{\mathrm{L}}, \vec{J}_{\mathrm{R}'} = \vec{P}_\psi \vec{J}_{\mathrm{R}}, \end{gathered} \tag{7}$$

$A(\psi, \alpha')$ and $\xi(\psi, \alpha')$ are defined as [8]. Fringe contrast m_{qr} is represented by

$$m_{qr} = \frac{2J_q J_{q+1}}{J_q^2 + J_{q+1}^2}, \tag{8}$$

where each fringe contrast depends on the relative phases between the Bessel functions J_q. The Fourier spectrum of the grid in our tests behaves as sketched in figure 2. Contrast is positive for one half of the diffraction orders if the grating's Fourier coefficients are all positive for $q > 0$, whereas the other half will show alternating contrasts due to the odd parity of J_{2q+1}. These results can also be depicted as in figure 2, where two equal phase gratings with their respective $+4$th diffraction order are assumed to be negative; thus, the -4th diffraction order turns out also to be negative (see figure 2(a)). A phase grid is formed with two gratings at 90°, and the resulting Fourier spectrum forms a rectangular reticule (see figure 2(b)) [19]; then, there are orders pointing out of the plane of the paper (circles) and others pointing in the opposite direction (crosses).

This means that there is a phase difference between such orders when they interfere: some orders are in phase (dots with dots or crosses with crosses, but only one symbol of these is depicted), and others are out of phase (dots with crosses). The respective contrast of each resulting interference pattern depends on the relative phases between the Bessel orders J_q, so the presence of only one symbol represents positive contrast, while the presence of both symbols represents a reversal of contrast. On the image plane, an interference pattern between the fields associated with each window must appear within each replicated window shifted by an amount ξ induced by polarization.

3.1. 2D interference patterns generated by diffraction

The interference patterns are obtained from the interference between the replicas of each beam, centered around each diffraction order. Figure 3(a) presents the replicas of beam A, with right circular polarization, and the replicas of beam B, with left circular polarization; each order is superposed depending on separation x_0 of the beams at the output of the MZ system. Figure 3(b) presents the interference pattern generated by the interference of contiguous orders $[(-1, -2), (0, -1), (+1, 0), (+2, +1)]$, where $x_0 \cong 8$ mm. Due to the capability of the system to change the separation

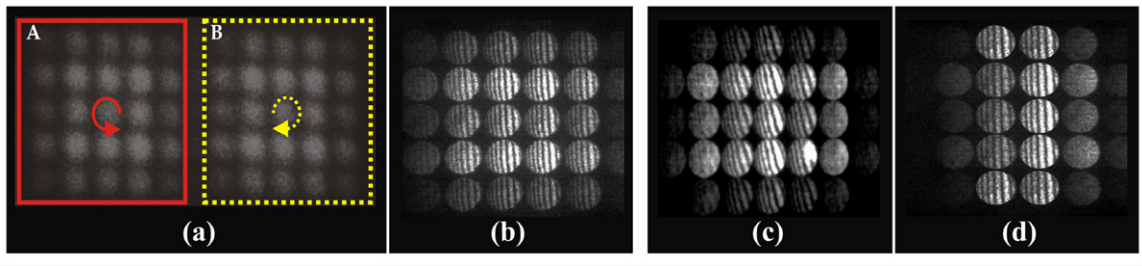

Figure 3. Replicated beam generated through phase grating. (a) Replicas of beams A (continuous rectangle) and B (dotted rectangle). (b) Interference pattern obtained by means of the order diffraction superposition presented in figure 2 (contiguous orders) for $x_0 \cong 8$ mm. By changing beam separation, we can properly interfere different order diffractions (c) $x_0 \cong 1.8$ mm and (d) $x_0 \cong 2.6$ mm.

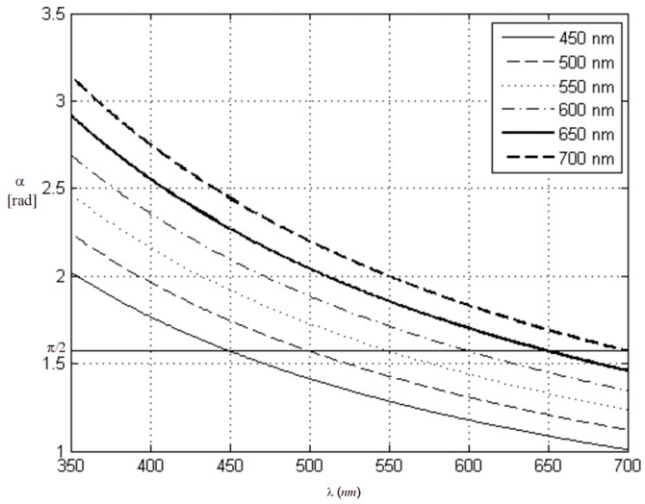

Figure 4. Dependence of retardation (α') on wavelength λ for different birefringent wave plates.

of the beams, we also present the interference pattern generated by other diffraction orders. Figure 3(c) presents the interference pattern generated by the interference of orders $[(-2, 0), (-1, +1), (0, +2)]$ with $x_0 \cong 1.8$ mm, and in figure 3(d) we also present order superposition $[(+1, -2), (+2, -1)]$ with $x_0 \cong 2.6$ mm. Varying the beam separation (x_0) allows the interference of orders of equal amplitude, resulting in interference patterns of equal intensity and equal modulation used for the processing of the phase data. It can be seen that by using more distant orders, the interference pattern number decreases due to the fringe contrast decrement caused by the modulation obtained by the Bessel function of the diffraction spectrum of the phase grid used.

For convenience, the experimental results presented in this work were retrieved through the use of contiguous order interference only, figure 3(b).

3.2. Phase shifts for inexact retardation

Figure 4 shows the dependence of retardation (α') on wavelength λ for different birefringent wave plates. This result shows that retardation is not a linear function of wavelength, i.e. $\alpha'(\lambda) = \frac{\pi}{2}\frac{\lambda_0}{\lambda}$, with λ_0 being the operating wavelength of the QWP, and λ the wavelength of the laser used; so the retardation for $\pi/2$ has to work with the correct wavelength shown in the graph, where the horizontal line shows the case of $\alpha' = \frac{\pi}{2}$. Representing the case of exact quarter-wave retardation, it is readily found that $\xi(\psi, \frac{\pi}{2}) = 2\psi$, $A^2(\psi, \frac{\pi}{2}) = 1$.

Experimentally, phase shifting results after applying a linear polarizer to each one of the interference patterns generated around each diffracting order at the exit plane (P_i). Each polarizing filter transmission axis is adjusted at a different angle ψ_i (see figure 5). Experimental observations suggest a simplification for the polarizing filter array; thus, it is not necessary to use all linear polarizing filters for all patterns; only two polarizers (P_0 and P_1) need to be placed, each one covering two patterns with complementary phase shifts. Then, $\psi_0 = 0°$ and $\psi_1 = 46.577°$, which leads to phase shifts ξ of, $0, \pi/2, \pi$, and $3\pi/2$; this can be seen in figure 5, where the dotted boxes represent the polarizing filters.

4. Phase objects

A phase object (transparent) that is placed onto beam B can be expressed as:

$$O(x, y) = 1 + \mathrm{i} \cdot \phi(x, y); \tag{9}$$

using this approach for thin phase objects where $|\phi(x, y)|^2 \ll 1$, it can be noted that the phase of the object is proportional to the function that defines its shape. This way, we can know the profile of the object by analyzing the optical phase; phase reconstruction is performed using a four-step phase shifting algorithm [17, 20, 21], so the phase can be obtained from the following equation:

$$\phi(x, y) = \tan^{-1}\left(\frac{I_1 - I_3}{I_2 - I_4}\right) \tag{10}$$

with I_i being the intensity measurements captured in a single shot, with the values of ψ given by $\psi_0 = 0°$, $\psi_1 = 46.577°$. Applying the techniques of unwrapped phase to equation (10), the profile of a thin phase object is:

$$O(x, y) = 1 + \mathrm{i} \cdot \mathrm{unwrap}[\phi(x, y)]. \tag{11}$$

This result allows us to know the object's profile. Since n-interferograms can be obtained simultaneously, the dynamic study of a phase object can be carried out.

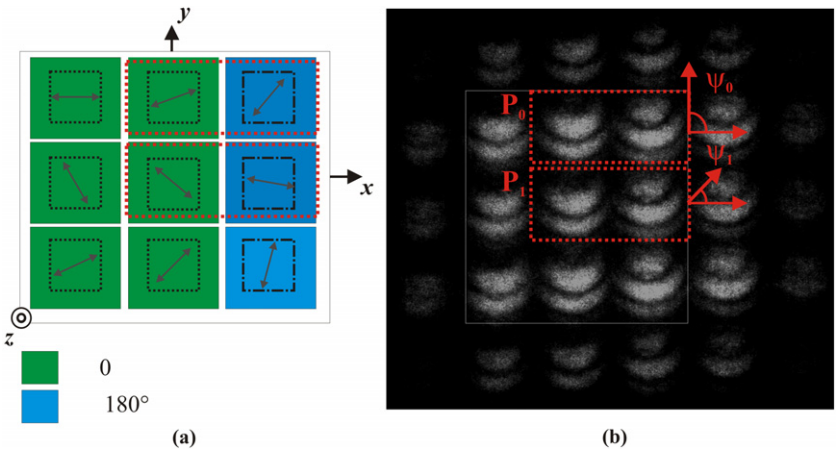

Figure 5. Replicas of the interference patterns obtained with the phase grid with π-phase shifts. (a) Polarizing filter array. (b) Experimental interference patterns.

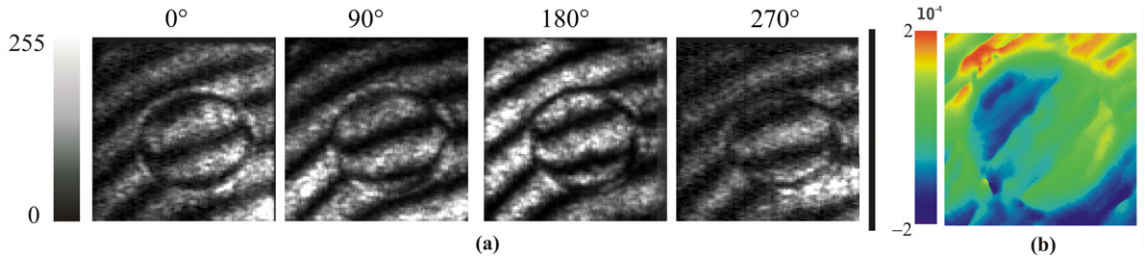

Figure 6. Static object: phase dot. (a) Interference patterns. (b) Unwrapped phase.

5. Experimental results

The phase gratings that were used are commercially available ones, which are nominally identical according to the seller (Edmund Optics transmission grating; dimensions 25 × 25 mm^2; dimensional tolerance $\pm$0.5 mm; substrate, optical crown glass). By taking the phase shifting error as $\delta\xi \cong 2\delta\psi$, and no variation in the measuring field, we use conventional phase shifting algorithms to retrieve the phase data map [22]. For the experimental results presented, we used a monochromatic camera (CMOS) with 1280 pixels × 1024 pixels. Each pattern was filtered using a conventional low-pass filter to remove sharp edges and details. To reduce differences of irradiance and fringe modulation, every interferogram used was subjected to a rescaling and normalization process. This procedure generates patterns of equal intensities and equal fringe modulation.

A phase dot was placed in the path of beam B, while beam A was used as a reference; the results obtained are shown in figure 6. Figure 6(a) shows the four patterns obtained in a single shot, and figure 6(b) presents the profile of the phase object in false color coding.

Figure 7 shows the case of moving distributions. The upper row corresponds to flowing water on a microscope slide, and it shows the profile resulting from phase evolution $\phi(x, y, t)$ (media 1 available at stacks.iop.org/JOpt/13/115502/mmedia). The lower row shows oil on a microscope slide, it shows the temporal evolution of the oil flow (media 2 available at stacks.iop.org/JOpt/13/115502/mmedia), clearly showing the phase changes induced by the oil. Figure 8 shows the results for oil drops on microscope slides; the evolution of the drops as they cross in front of the camera can be shown. Images are presented in 4D [21] (media 3 available at stacks.iop.org/JOpt/13/115502/mmedia).

5.1. Automated capture and phase data processing

In order to automate image capture and process the phase, we developed a program called Dynamic Phase V.1 [23] using Labview 8.5. The main purpose of the program is to demodulate the fringe patterns generated by the optical system using the conventional four-step phase shifting method. The four interferograms retrieved have relative $\pi/2$ phase shifts generated simultaneously and distributed in a four-quadrant image.

The configuration of our program starts by using an iris diaphragm to locate a common zone of the interference replicas used as a reference points (figure 9(a)); this procedure locates each centroid of the points shot by the camera that belong to the shifted interference patterns used. After locating each reference point, a geometric mask (rectangle, ellipse, polygons, etc) is selected in the program, taking into account the first centroid, to obtain the common interference pattern region. Through this procedure, our program is capable of selecting the four interference pattern locations, and by using digital image

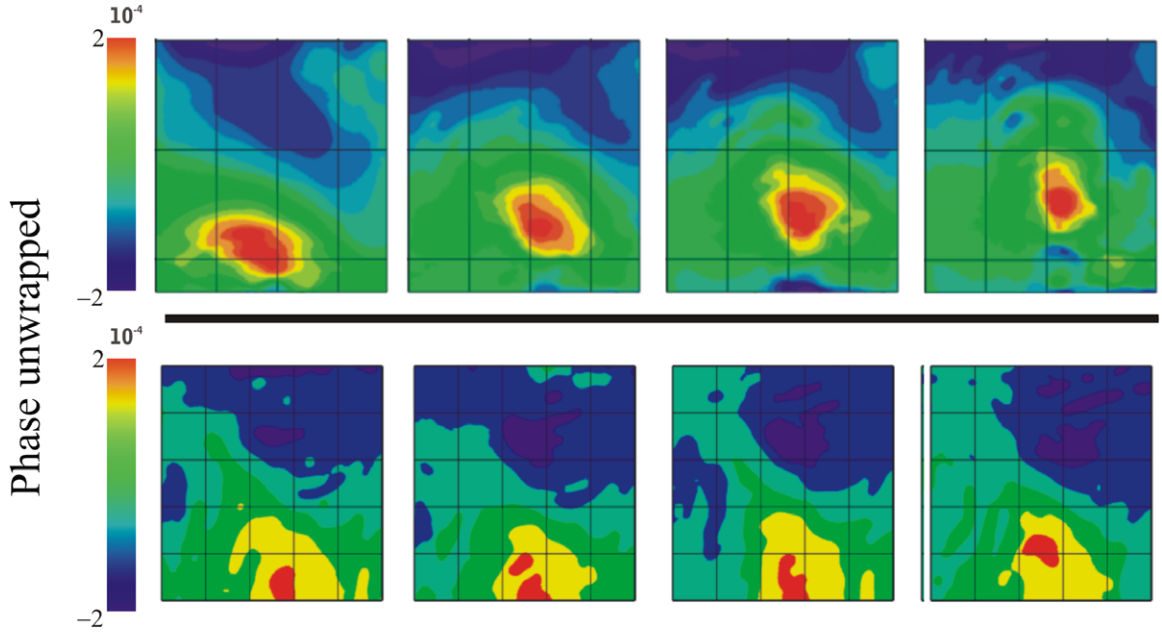

Figure 7. Dynamic distributions. Representative frames. Evolution of the phase. Upper row: flowing water on a microscope slide (media 1 available at stacks.iop.org/JOpt/13/115502/mmedia). Lower row: oil on a microscope slide (media 2 available atstacks.iop.org/JOpt/13/115502/mmedia). One capture per second.

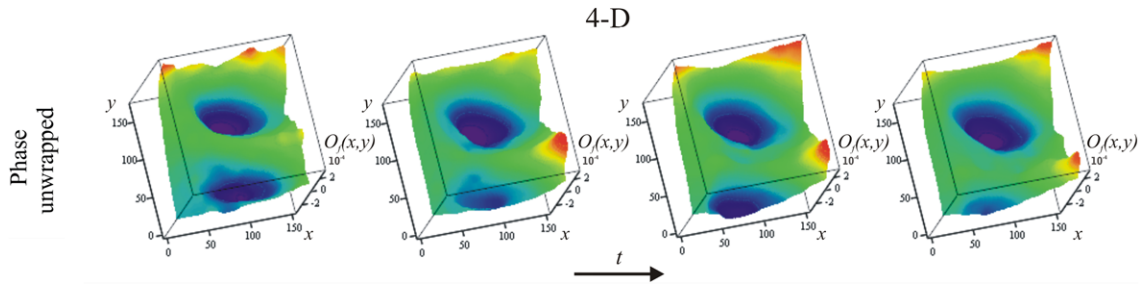

Figure 8. Immersion oil on a microscope slide. Oil drops moving under gravity on a slide (media 3 available atstacks.iop.org/JOpt/13/115502/mmedia). One capture per second.

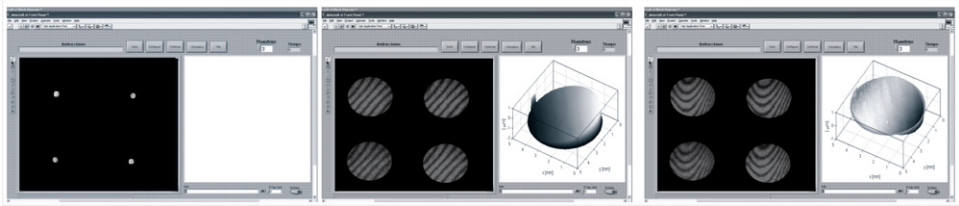

Figure 9. Platform used to automate the phase data processing. (a) Selected the centroids of each interferograms. (b) The phase reference. (c) Phase of the object under study.

processing filters in each interferogram, we obtain the wrapped phase data.

The method used to unwrap the phase data was a quality-guided path following method [24]. In order to obtain the optical phase, first a reference phase map is taken (see figure 9(b)), to be subtracted with the phase map of the object in each capture. This is shown in figure 9(c). We are capable of capturing one image every 100 ms with a resolution of 480 pixels × 480 pixels.

Figure 10 shows the DynamicPhase V.1 platform based on a Labview structure. The program allows dynamic phase measurements by imaging the four shifted interferograms in a single capture. In this case, we present the temporal phase evolution of a thin flame candle (media 4 available at stacks.iop.org/JOpt/13/115502/mmedia). These results show that dynamic phase objects can be analyzed with the optical system used.

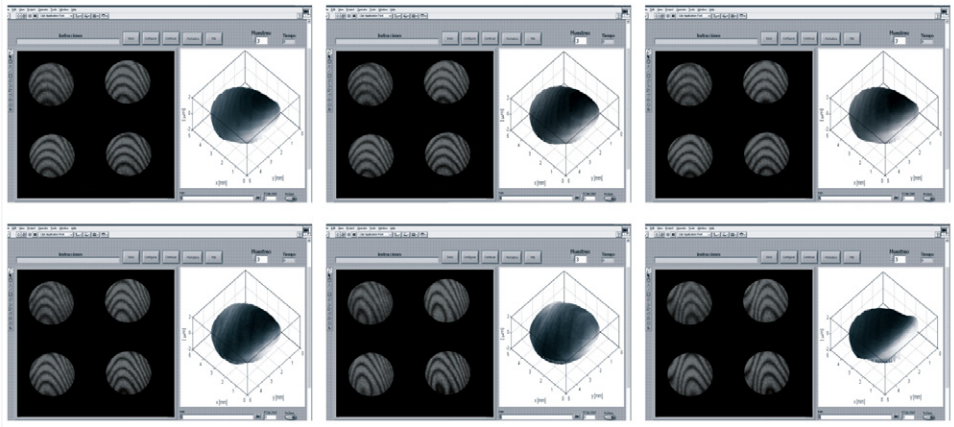

Figure 10. 4D Phase profile measurement. Representative capture of the developed program used for phase data processing (media 4 available at stacks.iop.org/JOpt/13/115502/mmedia).

6. Final remarks

The experimental setup for a simultaneous phase shifting quasi-common-path interferometer based on a Mach–Zehnder system has been described to obtain the profiles of phase objects from theanalysis of optical phase using phase shifting techniques. This system is able to obtain several interferograms simultaneously. One of the primary characteristics of the system presented is the adjustable beam separation with the combination of the phase shift generated for the grating, thus simplifying the polarizing filter array used. This characteristic optimizes the interferometric system used and allows the analysis of static and dynamic phase objects by using an automated phase data processing platform briefly introduced, allowing 4D phase profile measurement of phase objects.

Acknowledgments

The authors thank M A Ruiz for his contribution in proofreading the manuscript. The experimental results are part of the bilateral projects between Mexico–Chile (CONACYT–CONICYT) and Mexico–Italy (CONACYT–MAE). Partial support from 'Consejo Nacional de Ciencia y Tecnología (CONACYT)' and 'Centro de Investigaciones en Óptica AC (CIO), project 290597 (CONACYT–CIO), and from Benemérita Universidad Autónoma de Puebla (BUAP), project 154984 (CONACYT–BUAP) is also acknowledged.

N-IT-A expresses sincere appreciation to Luisa, Miguel and Damian for the support provided, and to CONACYT for grant 102137/43055. DIS-G (grant: 227470/31458) is very grateful to CONACyT for the graduate scholarship granted, and expresses sincere appreciation to Geliztle.

References

[1] Hu H Z 1983 Polarization heterodyne interferometry using a simple rotating analyzer.1: theory and error analysis *Appl. Opt.* **22** 2052–6

[2] Liu J P and Poon T C 2009 Two-step-only quadrature phase-shifting digital holography *Opt. Lett.* **34** 250–2

[3] Yamaguchi I and Zhang T 1997 Phase-shifting digital holography *Opt. Lett.* **22** 1268–70

[4] Yamaguchi I, Kato J, Ohta S and Mizuno J 2001 Image formation in phase-shifting digital holography and applications to microscopy *Appl. Opt.* **40** 6177–86

[5] Nakadate S and Saito H 1985 Fringe scanning speckle-pattern interferometry *Appl. Opt.* **24** 2172–80

[6] Ferrari J A, Frins E M and Perciante C D 2002 A new scheme for phase-shifting ESPI using polarized light *Opt. Commun.* **202** 233–7

[7] Bruning J H, Herriott D R, Gallagher J E, Rosenfeld D P, White A D and Brangaccio D J 1974 Digital wavefront measuring interferometer for testing optical surfaces and lenses *Appl. Opt.* **13** 2693–703

[8] Griffin W D 2001 Phase-shifting shearing interferometer *Opt. Lett.* **26** 140–1

[9] Kothiyal M P and Delisle C 1985 Shearing interferometer for phase shifting interferometry with polarization phase shifter *Appl. Opt.* **24** 4439–42

[10] Rodriguez-Zurita G, Meneses-Fabian C, Toto-Arellano N-I, Vázquez-Castillo J F and Robledo-Sánchez C 2008 One-shot phase-shifting phase-grating interferometry with modulation of polarization: case of four interferograms *Opt. Express* **16** 7806–17

[11] Rodriguez-Zurita G *et al* 2009 Adjustable lateral-shear single-shot phase-shifting interferometry for moving phase distributions *Meas. Sci. Technol.* **20** 115902

[12] Rodriguez-Zurita G, Toto-Arellano N-I, Meneses-Fabian C and Vázquez-Castillo J F 2008 One-shot phase-shifting interferometry: five, seven, and nine interferograms *Opt. Lett.* **33** 2788–90

[13] Meneses-Fabian C *et al* 2009 Phase-shifting interferometry with four interferograms using linear polarization modulation and a Ronchi grating displaced by only a small unknown amount *Opt. Commun.* **282** 3063–8

[14] Toto-Arellano N-I, Martínez-García A, Rodríguez-Zurita G, Rayas-Álvarez J A and Montes-Perez A 2010 Slope measurement of a phase object using a polarizing phase-shifting high-frequency Ronchi grating interferometer *Appl. Opt.* **49** 6402–8

[15] Serrano-García D I, Toto-Arellano N-I, Martínez García A, Rayas Álvarez J A, Téllez-Quiñones A and Rodríguez-Zurita G 2011 Simultaneous phase-shifting cyclic interferometer for generation of lateral and radial shear *Rev. Mex. Fís.* **57** 0255

[16] Novak M, Millerd J, Brock N, North-Morris M, Hayes J and Wyant J 2005 Analysis of a micropolarizer array-based simultaneous phase-shifting interferometer *Appl. Opt.* **44** 6861–8

[17] Barrientos-García B, Moore A J, Pérez-López C, Wang L and Tschudi T 1999 Transient deformation measurement with electronic speckle pattern interferometry by use of a holographic optical element for spatial phase stepping *Appl. Opt.* **38** 5944–7

[18] Barrientos-García B, Moore A J, Pérez-López C, Wang L and Tschudi T 1999 Spatial phase-stepped interferometry using a holographic optical element *Opt. Eng.* **38** 2069–74

[19] Toto-Arellano N I, Rodriguez-Zurita G, Meneses-Fabian C, Vázquez-Castillo J and Robledo-Sánchez C 2008 Phase shifts in the Fourier spectra of phase gratings and phase grids: an application for one-shot phase-shifting interferometry *Opt. Express* **16** 19330–41

[20] Malacara D, Servin M and Malacara Z 2005 Phase detection algorithms *Interferogram Analysis for Optical Testing* (Taylor & Francis) chapter 6

[21] Wyant J C 2003 Dynamic interferometry *Opt. Photon. News* **14** 36–41

[22] Surrel Y 2000 Fringe analysis *Photomechanics Top. Appl. Phys.* **77** 55–102

[23] Rayas-Álvarez J A, Toto-Arellano N I, Serrano-García D I and Martinez-García A 2011 DynamicPhase v.1, software developed by J A Rayas-Álvarez *etal*, CIO, León, Gto, México

[24] Ghiglia C and Pritt M D 1998 *Two-dimensional Phase Unwrapping: Theory, Algorithms, and Software* (New York: Wiley) chapter 4